nature portfolio

Peer Review File

Three-dimensional atomic insights into the metal-oxide interface in Zr-ZrO2 nanoparticles

REVIEWER COMMENTS

Reviewer #1 (Remarks to the Author):

Y. Zhang et al have reported on the 3D structural analysis of Zr/ZrO2 nanoparticles using atomic-resolution electron tomography. The present topic is important and should be of wide interest to the scientific community, including electron microscopy and materials science. Several issues need to be addressed before I can fully support the publication.

– The reviewer expected that the atomic packing density of a-ZrO2 might be smaller than that of c-ZrO2. However, there is no significant difference between these phases. Is there any clear description origin on this matter?

– How did the author calibrate the distance of the atomic-resolution images without known structures? The scanned images are usually distorted and each scanned image (different tilt) could have different distortion.

– According to the experimental detector geometry, the inner angle of the ADF is relatively small. Therefore, oxygen atoms could also contribute to the image contrast. Did the authors consider the contrast contribution of the oxygen atoms, especially in the a-ZrO2 region?

– The authors have studied the spatial distribution of Zr vacancies and nanopores. However, it is still unclear the origin of the separation into two phases of a-ZrO2 and c-ZrO2. It would be nice if the authors could clarify the origin of the formation of two phases rather than single c-ZrO2 formation.

– In the opinion of the reviewer, it is not so easy to fill the Zr lattice with oxygen atoms. This is because the distribution of ρN is relatively broad even for c-ZrO2, and in addition, the BOO (Fig. 1b) also shows a broad spectrum. How to validate the current oxygen atom filling? Why does the oxidation degree is non-uniform, as shown in Fig. 2e?

Reviewer #2 (Remarks to the Author):
None.

Reviewer #3 (Remarks to the Author):

The work by Zhang et al reconstruct a Zr-ZrO2 nanoparticle in 3D at atomic resolution using electron tomography with atom location filtering (a method known as atomic electron tomography, AET). This challenging technique allows the authors to study the interface between the metal and metal-oxide with atomic specificity.

The figures and analysis are well presented and new results in atomic resolution electron tomography remain at the forefront of modern science. However, AET relies heavily on post reconstruction filtering to identify atom sites. This often uses human discretion and prior assumptions about atomic structure — which may be reasonable, but this manuscript is far too scant on the details to assess. Because the limitations and accuracy of AET has yet to be determined the authors should maintain high reproducibility.

The authors need to provide substantial details in order to properly review this manuscript. Further review is merited because the quality of the results are promising and of broad interest to readers at Nature. Overall, I support this work with a strong request for more experimental details and validation.

=Reproducibility=
(1) AET requires significant post processing. In addition to providing the filtering code, the authors should report how many atoms were removed by hand (Line 395: Typically <1% is not specific). In particular, the authors are assessing interfaces where filtering and prior knowledge methods are most likely to fail.

(2) Authors choose a 2 Angstrom cutoff to remove atoms from the reconstruction. This number is not explained, especially given that oxygen sites are ignored in the reconstruction. These details are the key aspects of this work.

(3) The authors should show the raw reconstructions in the supplemental and provide the data before and after reconstruction. The raw reconstruction needs to be provided for assessment.

(4) Line 110: It is not appropriate to cite other tomography manuscripts for your reconstruction methods. This manuscripts novelty is primarily in the data and reconstruction, less about the scientific conclusions around ZrO.

=Reconstruction Accuracy=
(5) The authors should analyze the raw reconstructions to show consistency with the wire diagrams in Fig 3. The interpretation of these interfaces should be clearly visible from the raw reconstruction.

(6) Atomic electron tomography suffers severely from the lack of full specimen tilt known as the missing wedge. This work has a typical missing wedge which will prevent accurate reconstruction on regions of this nanoparticle. Attempts to alleviate this have been done with machine learning (https://www.nature.com/articles/s41467-021-22204-1), however those bring in unwanted prior assumptions about crystal structure. It is not clear to the reader what parts of the atoms presented can be reliably analyzed.

(7) The authors present as though all atoms have been accurately reconstructed. However, it may be that 80-90% of the atoms are correctly identified with false positives and false negatives present. The reader will incorrectly assume that AET provides 100% accuracy. Rather, readers should understand that this accuracy is marked achievement for directly measuring atomic structure in matter.

=Self Consistency with EELS / EDX=

(8) The reconstructions seem inconsistent with the core-shell structure in S Fig1, 3. The most convincing reconstruction would be a crystalline metal core and a mostly / partially amorphous oxide shell. Why are the S. Fig1, 3 so different than the reconstructed particles (note the raw projection data in S Fig 4,5,6 do not have the same structure as S. Fig1, 3 so they may be a different type of particle).

(9) Authors claim to map oxygen indirectly from the local volume around metal sites. This is an interesting approach, but I am not confident it provides the resolution accuracy to conclude that oxygen metal interfaces are gradually smooth. In fact, everything else in this manuscript suggests this is not the case (the crystal to amorphous transitions, and the chemical maps in SFig 3). Chemical mapping in projection can make these assessments reasonably well and they do not appear to be in agreement. It may be prudent to not overclaim the accuracy of oxygen mapping using this method.

(10) Authors do not explain why the oxygen sites are not reconstructed. The signal from the MAADF is lower, but some oxygen scattering still occurs. Discussion here would be helpful.

(11) In Figure 4, the authors analyze voids from what appears to be the raw reconstruction. This is the correct approach. However, it is not clear if this is in fact the raw reconstruction, or if it is a reconstruction made after atoms were filtered out using the atom tracing methods. Also, is oxygen

present in these voids?

=Other=

(12) The manuscript incorrectly claims to use HAADF imaging. However, the requirements for HAADF are inner collection angles 3x the convergence angle (see H. Rose). At 1.5x the convergence angle this would be medium angle ADF (MAADF). The artifacts associated with MAADF AET remain poorly known. It is unlikely to change the primary conclusions of the manuscript, but will reduce the total number of accurately reconstructed atom sites.

=Minor comments=

+ Authors claim on Line 373, "5E5 e/A^2 is a very low dose rate" however, this is far from low dose exposures to materials. For tomographic imaging, it is about average and on par with other AET work, more broadly it would be considered higher dose.

There are several minor grammatical / writing comments that are easily corrected. They do not detract from the scientific merit of this work.

Line 32: The first sentence here should be removed.
Line 35: "oxidation processes"
Line 38: "the" Kirkendall effect
Line 43: Do the authors intend to say observation of theories? The theories are aften atomistic.
Line 64: "is limited to"
Line 66: "difficult to image"
Line 77: "tomography experiments"
Line 73: Should be "chose" not "choose"

Response to Reviewer #1:

Y. Zhang et al have reported on the 3D structural analysis of Zr/ZrO_2 nanoparticles using atomic-resolution electron tomography. The present topic is important and should be of wide interest to the scientific community, including electron microscopy and materials science. Several issues need to be addressed before I can fully support the publication.

Comment 1: *The reviewer expected that the atomic packing density of a-ZrO_2 might be smaller than that of c-ZrO_2. However, there is no significant difference between these phases. Is there any clear description origin on this matter?*

Response: We would like to clarify this important point. Amorphous ZrO_2 (a-ZrO_2) has a wide range of density distribution. The atomic packing density (ρ_N) of a-ZrO_2 ranges from 2.12×10^{-2} to 2.91×10^{-2} Å^{-3} (4.34 g/cm^3 to 5.96 g/cm^3), as reported by previous DFT simulation results (Vanderbilt, D. *et al*. *Thin Solid Films* **486**, 125–128 (2005); Ceresoli, D. *et al*. *Phys. Rev. B* **74**, 125108 (2006)) and experimental results (Koyama, S. *et al*. *Electrochim. Acta* **55**, 3144–3151 (2010)). Our AET results show the averaged local ρ_N of a-ZrO_2 in Zr1 particle is 2.89×10^{-2} Å^3 (5.92 g/cm^3), which is in the reported range of density in a-ZrO_2. We want to point out that some of the Zr particles including Zr1 are not fully oxidized; some partially oxidation regions in a particular nanoparticle may have a higher ρ_N. This agrees with our 3D oxygen filling maps of Zr1 in which the oxidation states are non-uniform and some regions are partially oxidized (Fig. 2e).

The density of the oxide region depends on whether the particle is fully oxidized. We also calculated the density of the a-ZrO_2 in two other ZrO_2 particles (Zr2 and Zr3) which are fully oxidized (Fig. R1, Supplementary Fig. 14). Using the same density calculation method, we obtained the ρ_N of the entire a-ZrO_2 regions in Zr2 and Zr3 being 2.65×10^{-2} Å^{-3} (5.32 g/cm^3) and 2.62×10^{-2} Å^{-3} (5.26 g/cm^3), respectively. The ρ_N of the fully oxidized a-ZrO_2 is indeed smaller than that of c-ZrO_2 from our measurement.

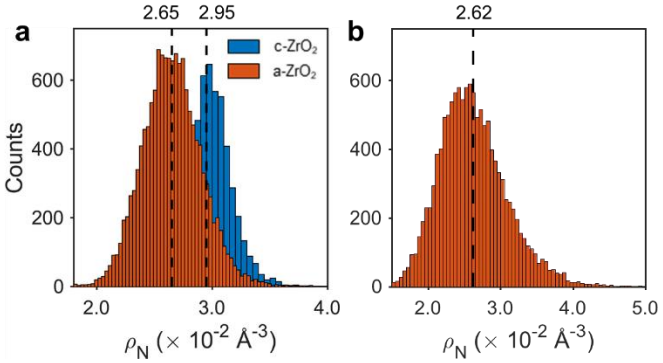

Figure R1. Distribution of ρ_N in Zr2 and Zr3. a, The ρ_N distribution of c-ZrO_2 (blue), a-ZrO_2 (red) phase in Zr2. The a-ZrO_2 and c-ZrO_2 have mean ρ_N distributions of 2.65×10^{-2} Å^{-3} and 2.95×10^{-2} Å^{-3} (dashed lines), respectively. **b**, The ρ_N distribution of a-ZrO_2 phase in Zr3. The a-ZrO_2 has mean ρ_N distributions of 2.62×10^{-2} Å^{-3} (dashed line).

Comment 2: *How did the author calibrate the distance of the atomic-resolution images without known structures? The scanned images are usually distorted and each scanned image (different tilt) could have different distortion.*

Response: Our microscope has a ~4% error in nominal pixel size provided by the manufacturer. This is common when the pixel size of a microscope is not well calibrated. We have used a standard crystalline sample, a cubic structured monocrystalline Si to calibrate the pixel size of the electron microscope.

The calibration procedures are shown in Fig. R2. The FIB sample of silicon is rotated to the [110] zone axis. Calibration images are taken at the same magnification with the same pixel size as the tomography experiments (The nominal pixel size is 35.8 pm for 512 × 512 image at 5.1 × 10^6 magnification). In order to correct any potential image distortion caused by sample drift, we take 20 to 50 frames for each image. The dwell time of one pixel in each frame is from 200 to 500 μs, which significantly alleviates the image distortion due to the drift. For each image, all frames are aligned and then averaged. The brightest spots of the fast Fourier transform (FFT) are precisely located using 2D gaussian fit. The distances of these points to the center of FFT are the countdowns of the lattice spacing of the image in the real space. Thus, we can get the lattice constants measured in this image. By comparing it to the standard lattice constants of Si, we can calibrate the pixel size at this magnification. We take multiple Si images at different scan rotation angles and then determine the mean value of the real pixel size (34.34 pm).

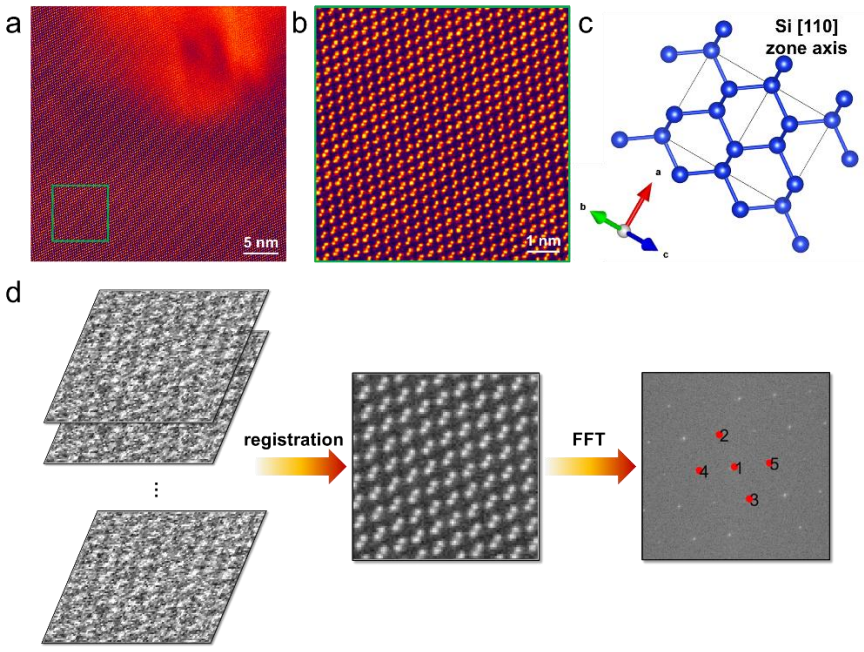

Figure R2. Calibration of the pixel size for the ADF-STEM images. a, ADF-STEM image of Si [110] zone axis. **b**, Magnified image of the green box in **a**. **c**, Crystal structure of cubic structured Si projected along [110] zone axis. **d**, Image processing procedure including registration and fast Fourier transform. The lattice spacing is measured based on the distance of point 2-5 to the central

point 1.

In addition to pixel calibration, we did drift correction for our tomography tilt series images. The distortion of the scanned images is usually due to the drift of samples or instability of the stage. To compensate the drift, we have collected three sequential frames of images at each tilt angle at a dwell time of 2 to 4 μs. We computed the cross-correlation coefficient between the three images at the same tilt angle to estimate the drift direction and drift speed. Then, we recovered the images without drift by interpolating the raw images with drift-corrected pixel positions. This drift correction method has been used in many other image processing. (Li, Z. *et al. Nat. Commun.* **14**, 2934 (2023); Ophus, C. *et al. Ultramicroscopy* **162**, 1-9 (2016)).

By carefully doing the calibration and drift correction, we obtained a well aligned tilt series and then computed the 3D reconstruction. From the traced Zr positions in the final reconstructions, we obtained the peak positions in our calculated PDFs of c-ZrO_2 in Zr1 and Zr2; they match with the peak positions of standard c-ZrO_2 well (Fig. 1c), which suggests we have a faithful reconstruction.

We have added more details about drift correction and the pixel calibration in the Methods of our revised manuscript.

Comment 3: *According to the experimental detector geometry, the inner angle of the ADF is relatively small. Therefore, oxygen atoms could also contribute to the image contrast. Did the authors consider the contrast contribution of the oxygen atoms, especially in the a-ZrO_2 region?*

Response: We thank our referee for raising up this good point. To collect more scattered electrons and improve SNR, we have acquired our images at inner angles of 39.4 (Zr1) and 31.5 (Zr2&3) mrad which indeed are in the ADF range rather than in the HAADF range. Although the contrast of light element in ADF mode is larger than that of HAADF mode, we find oxygens are still too light, and our current imaging parameters are not sufficient enough to detect oxygen.

First, to show the contrast contribution of oxygen in 2D ADF-STEM images, we have constructed a model of ZrO_2 which is 8-nm-thick slab; and then performed the multi-slice simulation along the [100] zone axis using prismatic package (L. Rangel DaCosta, *et al. Micron* **151**, 103141 (2021)), as shown in Fig. R3a. The noise-free ADF-STEM image shows the oxygen column intensity is typically ~10% of the zirconium column intensity; Line profile and histogram of the oxygen contrast are shown in Fig. R3b and c, respectively. We also added Poisson noise at the electron dose (1200 e/Å^2) used in the simulation, which is similar to the electron dose under our experiment conditions. The simulated images are noisier and the contrasts of oxygen columns become even lower (Fig. R3d), making the column of oxygen atoms barely seen (Figs. R3e & 3f).

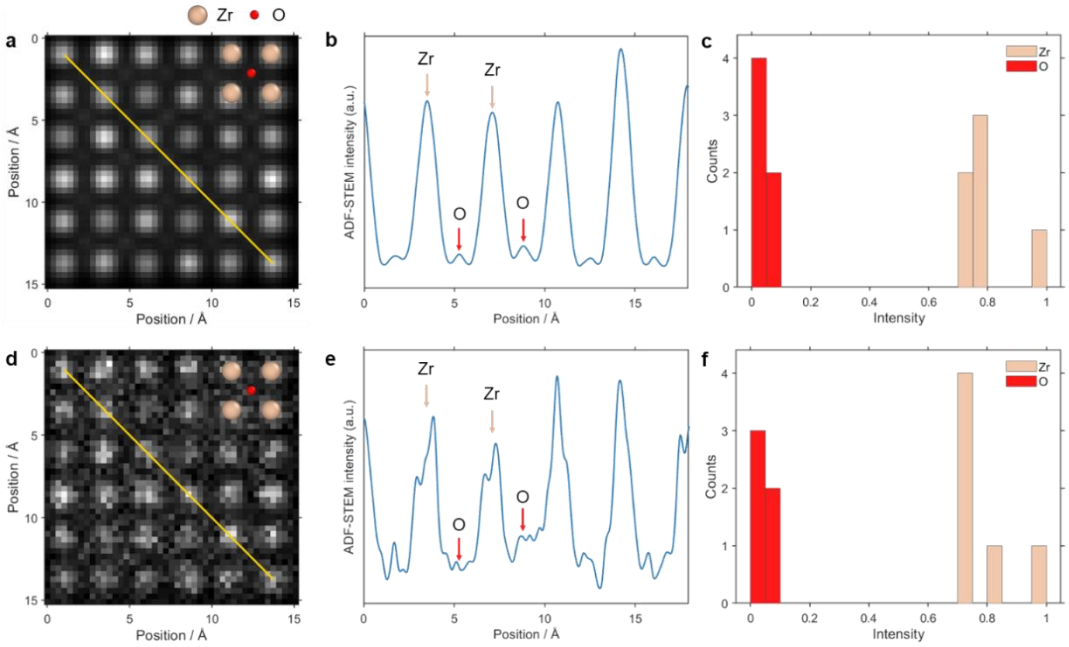

Figure R3. Multi-slice simulation of the ADF-STEM images of ZrO_2. a-c, Noise-free ADF-STEM image (**a**) of the 8-nm-thick c-ZrO_2 slab by multi-slice simulation along the [100] zone axis. The line profile (**b**) along the yellow line in panel **a** shows the intensity of Zr columns and O columns. The ivory arrows and red arrows show the position of Zr atoms and O atoms, respectively. (**c**) The intensity histograms of all Zr columns and O columns. The oxygen column intensity is typically 1/10 of the zirconium column intensity. **d-f**, Noise-added ADF-STEM image (**d**) of the 8-nm-thick c-ZrO_2 slab by multi-slice simulation along the [100] zone axis. The electron dose is determined according to the experimental conditions. The line profile (**e**) along the yellow line in panel **d** shows the intensity of Zr columns and O columns. The ivory arrows and red arrows show the position of Zr atoms and O atoms, respectively. The oxygen column contrast is much lower. (**f**) The intensity histograms of all Zr columns and O columns. In panel **a** & **d**, the Zr atoms and O atoms are colored in ivory and red, respectively. The parameters for the multi-slice simulation are listed in Supplementary Table 2. These simulation results show contrast of oxygen atoms is too light to be detected in 2D.

Second, to double check the contribution of oxygen atoms in 3D reconstruction, we have performed simulation of the tilt series and computed 3D reconstruction to show the oxygen contrast in 3D. The model for simulation (named Zr_S model) was built by filling oxygen atoms into the Zr1 experimental model (Fig. R4a). The oxygen atoms were filled in the eight tetrahedral sites (5.5 $Å^3$) of the oxide as described in the Methods section. We have performed multi-slice simulations to generate the same number of projections (Fig. R4b, parameters for simulations shown in Table R1) from the Zr_S model. By performing the same preprocessing, reconstruction, atom tracing and classification procedures, we obtained a multi-slice atomic model to check the contrast contribution of oxygen. Fig. R4c shows a representative c-ZrO_2 region, viewing from the [100] zone axis of the cubic ZrO_2. The corresponding 3D reconstructed volume and 3D surface rendering of all atoms are shown in Figs. R4d &

e, respectively. The cut-out of a-ZrO_2 is shown in Fig. R4f, along with the 3D reconstructed volume (Fig. R4g) and 3D surface rendering of all atoms (Fig. R4h). From either 3D reconstructed volume or traced atomic positions, we cannot distinguish the oxygen atoms in either c-ZrO_2 or a-ZrO_2 regions due to extremely low intensities/contrasts of the oxygen atoms. To further compare the intensities between Zr and O atoms in 3D, we analyzed the intensity distribution of Zr and O in our reconstructed volume, as shown in Figs. R4i & j. The intensities of Zr atoms are much higher than those of O atoms. The contrast/intensity contribution of oxygen atoms in 3D reconstructed volume is negligible for both c-ZrO_2 and a-ZrO_2. The oxygen cannot be traced correctly from the simulated reconstruction.

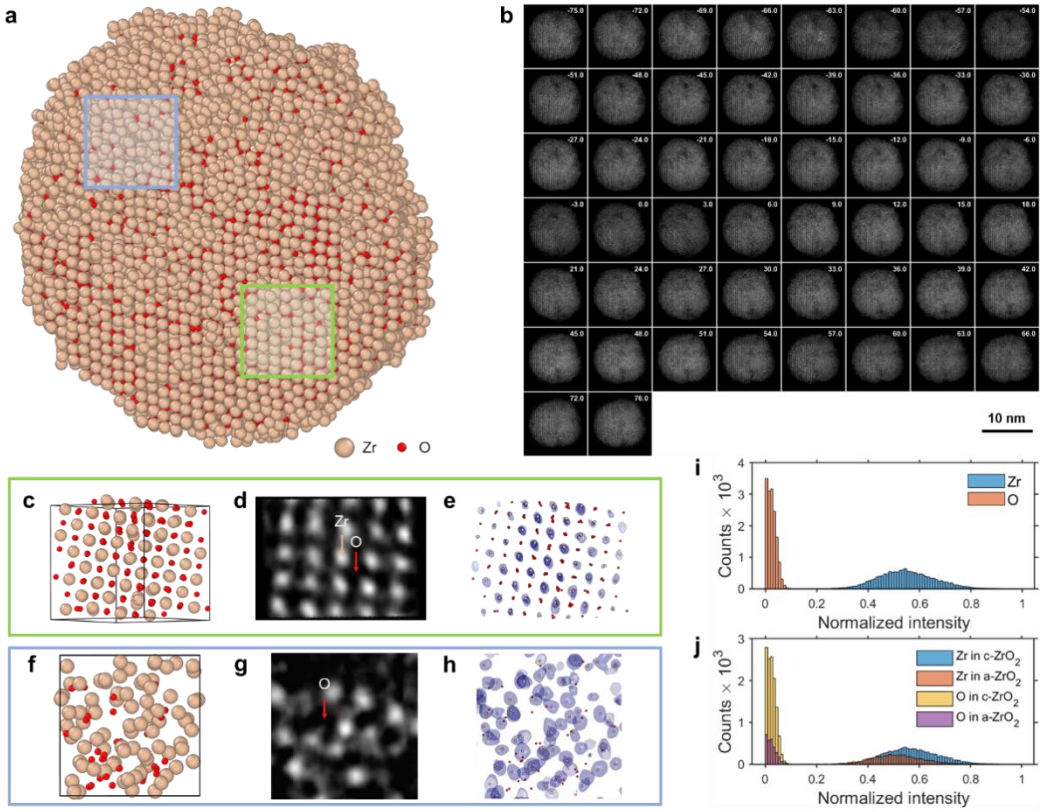

Figure R4. The 3D reconstruction obtained from the generated tilt series of the oxygen-filling atomic model. a, The atomic model for multi-slice simulation built by filling oxygen atoms into the Zr1 experimental model (Methods). **b**, The simulated tilt series with same number of projections to the experimental one in Supplementary Fig. 3, generated by the multi-slice simulation. **c-e**, A representative atomic cut-out from c-ZrO_2 region highlighted by the green square box in (**a**), viewing from the [100] zone axis of cubic ZrO_2. **c**, The atomic model of this representative c-ZrO_2 cut-out. The edge length of this cut-out is 15 Å. **d**, A 4-Å-thick slice from the corresponding 3D reconstructed volume. The ivory and red arrows show the positions of Zr and O atoms, respectively. **e**, 3D surface renderings of all the atoms in the specified cut-out, clearly indicating the intensity in oxygen positions are way too weak comparing to the Zr sites. The atom positions are displayed in this panel for a better comparison. **f-h**, A representative atomic cut-out from a-ZrO_2 region highlighted by the blue square box in (**a**). **f**, The atomic model of this representative a-ZrO_2 cut-out. The edge length of this cut-out is 15 Å. **g**, A 2.5-Å-thick slice

from the corresponding 3D reconstructed volume. The red arrow shows the position of an O atom. **h**, 3D surface renderings of all the atoms in the specified cut-out, clearly indicating the intensity in oxygen positions are way too weak comparing to the Zr sites. The atom positions are displayed in this panel for a better comparison. **i**, The intensity distribution of Zr and O atoms in the raw reconstructed volume. **j**, The intensity distribution of Zr and O atoms in a-ZrO_2 and c-ZrO_2 regions separately. In panel **a**, **c**, **e**, **f**, **h**, the Zr atoms and O atoms are colored in ivory and red, respectively. The parameters for the multi-slice simulation are listed in Supplementary Table 2. These simulation results show contrast of oxygen atoms is too light to be traced in 3D.

Table R1. Overview of multi-slice simulation settings.

Slice thickness	2 Å
Debye-Waller factor	0.3 $Å^2$
Acceleration voltage	300 kV
Convergence angle	30 mrad
Detector collection range	[39.4 – 200] mrad
FWHM of the point spread function	80 pm
Pixel size of simulated image	0.3434 Å
Pixel size to sample atomic potential	0.1 Å
Frozen phonons	4
Screen current*	30 pA

*The screen current is only applied for Figs. R3d & R4b and related analysis.

These results reveal the low contrast of oxygen atoms, both in 2D ADF-STEM images and 3D AET reconstruction. We have added these discussions in our revised manuscript.

Comment 4: *The authors have studied the spatial distribution of Zr vacancies and nanopores. However, it is still unclear the origin of the separation into two phases of a-ZrO_2 and c-ZrO_2. It would be nice if the authors could clarify the origin of the formation of two phases rather than single c-ZrO_2 formation.*

Response: In this study, we have employed a laser ablation method in ethanol to prepare the Zr nanoparticles. This technique can provide very high temperature to melt and vaporize metal target, and fast cooling to yield nanoparticles. However, the cooling rate for different regions in the liquid could vary a lot due to the thermal fluctuations. This could yield NPs with large variety of morphologies including amorphous, partially amorphous and crystalline metal nanoparticles (Liang, S.-X., *et al. Phys. Chem. Chem. Phys.* **23**, 11121–11154 (2021); Tong, X. *et al. Nat. Mater.* accepted (2024)). To check the oxidation state of the Zr NPs, we have synthesized fresh Zr NPs and prepared TEM samples right after laser ablation. We took many images of the obtained Zr NPs and found several kinds of heterogeneous structures including amorphous oxide, amorphous oxide containing crystal oxide core, amorphous oxide containing crystal metal core, and poly-crystal oxide, as Fig. R5 shows. The variety of heterogeneous structures is due to the fluctuation in cooling rate.

We speculate the amorphous oxide could originate from the amorphous Zr metal NP since a regular and stable Zr oxide form is in monoclinic crystal structure. The amorphous oxide and c-ZrO_2 are due to the relatively fierce fabrication process. From these results we could suggest that the large a-ZrO_2 and c-ZrO_2 grains in Zr1 could be the oxidation products of a heterogeneous Zr NP with amorphous and crystalline grains due to very fast cooling.

We also would like to point out that, our research interests focus on the 3D interface structure of Zr-ZrO_2 in this study. The origin of the separation into two phases of a-ZrO_2 and c-ZrO_2 is difficult to be directly revealed by current experiments. We are working on capturing the oxidation process of pure crystalline Zr NPs using chemical synthesis, we expect to provide solid results on the origin of possible a-ZrO_2 and c-ZrO_2 in another separated manuscript.

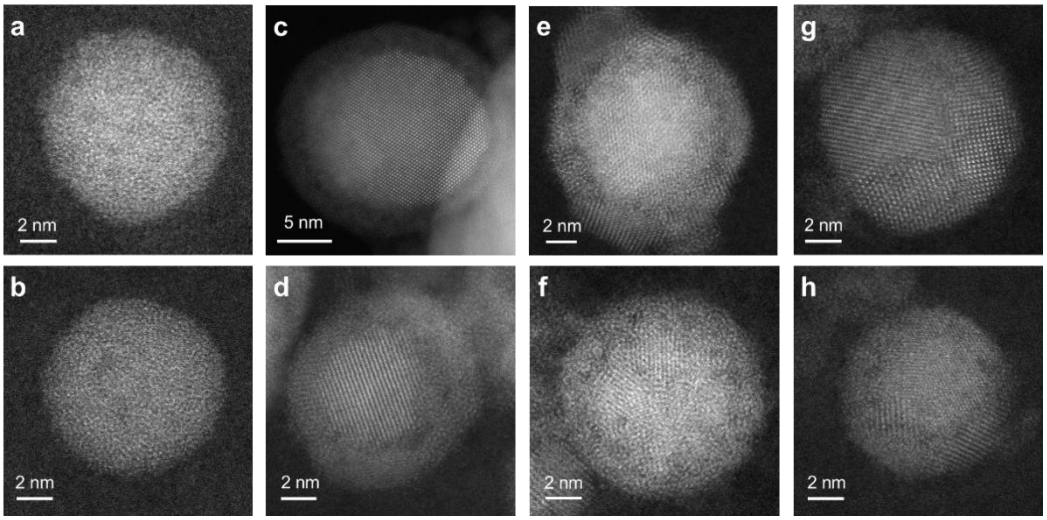

Figure R5. ADF-STEM images show the heterogeneous structures including amorphous oxide (**a**,**b**), amorphous oxide containing crystal oxide core (**c,d**), amorphous oxide containing crystal metal core (**e,f**), and poly-crystal oxide (**g,h**).

Comment 5: *In the opinion of the reviewer, it is not so easy to fill the Zr lattice with oxygen atoms. This is because the distribution of ρ_N is relatively broad even for c-ZrO_2, and in addition, the BOO (Fig. 1b) also shows a broad spectrum. How to validate the current oxygen atom filling? Why does the oxidation degree is non-uniform, as shown in Fig. 2e?*

Response: We would like to clarify this very important point. To further validate our oxygen filling method, we have performed iDPC-STEM imaging on a similar nanoparticle with a known structure, the cubic ZrO_2 phase. iDPC-STEM uses differential phase-contrast (DPC) imaging with the four-quadrant detector in STEM, and this technique provides improved sensitivity to light elements such as oxygens (Li, X. *et al. Adv. Mater.* **35**, 2207736 (2023)). Fig. R6a&b show the ADF and its corresponding iDPC images of a pure cubic ZrO_2 phase region. The images are consistent with the oxygen-filling structure visualized in Fig. R4c, viewing from the

[100] zone axis of cubic ZrO_2. Although the ADF-STEM and iDPC-STEM images on the zone axis of cubic ZrO_2 are projection images, we have obtained the information from the oxygen atomic column which is averaged through the thickness of the specimen.

We also would like to point out that our current oxygen filling is based on geometric frustration of the tetrahedra sites formed by Zr atoms. One prior assumption for this geometric frustration is as long as the volume of any tetrahedra site is large enough (4.68 $Å^3$), it would be filled with oxygen atoms. This assumption is based on a fact that Zr is a highly oxygenophilic metal, it is relatively easy to form Zr-O bonds to oxidize Zr metal. Although it cannot give us the precise information about where all the oxygen atoms exactly are, we believe it could still give us a fairly good estimation of the degree of oxidation based on the reasonable Zr-specific knowledge. This oxygen filling method can be further validated with our other two Zr particles. We have performed more analysis on the other two fully oxidized Zr NPs, Zr2 and Zr3. We have calculated the ρ_N and oxidation degree from the 3D reconstructions of Zr2 and Zr3. The two Zr NPs are almost fully oxidized and no metal core is observed (Supplementary Fig. 7). The oxidation maps of Zr2&3 show more uniform distribution of oxidation degree than that of Zr1 (Fig. R7). These results suggest our oxygen filling method is reasonable if the geometric frustration assumption stands.

There could be some heterogeneity in the degree of oxidation in some of the oxide grains, which makes the oxidation maps non-uniform. To further confirm the partial oxidation, we have done more experiments including EDS mapping and iDPC-STEM imaging. We have acquired EDS maps of many particles similar to Zr1 (Figs. R14 & R17), the oxygen maps show these particles are partially oxidized. The line profiles of iDPC images also validate the non-uniform oxygen filling in a cubic ZrO_2 grain, as Fig. R6c shows. The intensities of different oxygen columns are different.

We have added the more EDS mappings and iDPC results in the revised manuscript and have made some revisions to the oxygen filling method to make it clearer.

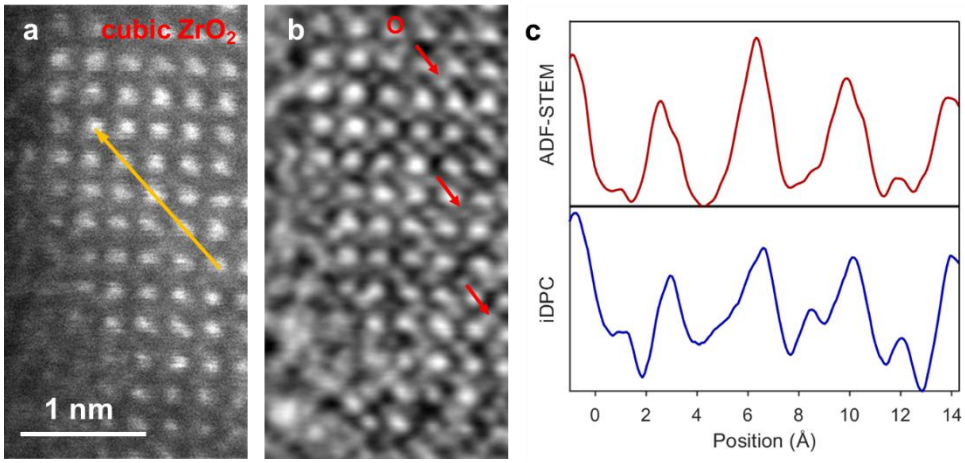

Figure R6. Partial Oxidation observed in Zr nanoparticle. The ADF-STEM image (**a**) and the

corresponding iDPC (**b**) image of the cubic ZrO_2 region in the nanoparticle, viewing along [100] zone axis. The red arrows mark the positions of oxygen atomic columns in the iDPC image. **c**, The line profile of ADF-STEM (up panel of **c**) and iDPC (down panel of **c**) images along the yellow arrow in panel **a**. The difference of oxygen intensities shows the non-uniform filling of oxygen atoms due to the partial oxidation of Zr NP.

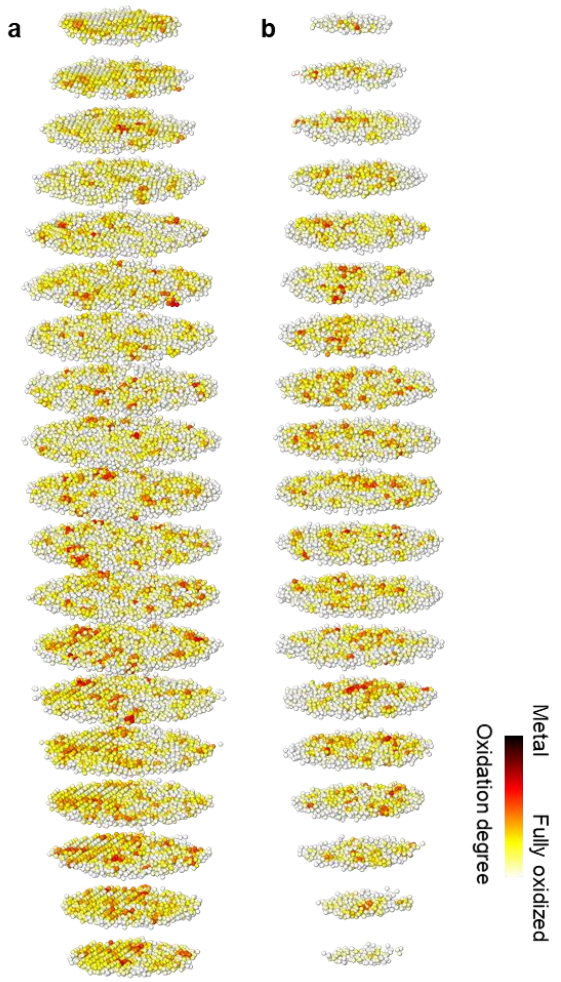

Figure R7. Oxidation degree of Zr2 and Zr3 nanoparticles. a, Atoms of the Zr2 NP colored according to the degree of oxidation, divided into slices with a thickness of 5.3 Å. **b**, Atoms of the Zr3 NP colored according to the degree of oxidation, divided into slices with a thickness of 5.3 Å. The Zr2 and Zr3 NPs are almost completely oxidized and have high degrees of oxidation comparing to Zr1 NP.

Response to Reviewer #3:

The work by Zhang et al reconstruct a Zr-ZrO_2 nanoparticle in 3D at atomic resolution using electron tomography with atom location filtering (a method known as atomic electron tomography, AET). This challenging technique allows the authors to study the interface between the metal and metal-oxide with atomic specificity.
The figures and analysis are well presented and new results in atomic resolution electron tomography remain at the forefront of modern science. However, AET relies heavily on post reconstruction filtering to identify atom sites. This often uses human discretion and prior assumptions about atomic structure — which may be reasonable, but this manuscript is far too scant on the details to assess. Because the limitations and accuracy of AET has yet to be determined the authors should maintain high reproducibility.
The authors need to provide substantial details in order to properly review this manuscript. Further review is merited because the quality of the results are promising and of broad interest to readers at Nature. Overall, I support this work with a strong request for more experimental details and validation.

=Reproducibility=
Comment 1: *AET requires significant post processing. In addition to providing the filtering code, the authors should report how many atoms were removed by hand (Line 395: Typically <1% is not specific). In particular, the authors are assessing interfaces where filtering and prior knowledge methods are most likely to fail.*

Response: We have uploaded our raw reconstructions (including the raw tilt series, raw reconstructions and traced atom positions along with all necessary codes) to Zenodo (https://doi.org/10.5281/zenodo.12742309). We have not used any filtering to trace the positions of atoms. Here is the procedure how we identify the atomic positions: first, we found the local maxima in the 3D reconstructions as potential atomic positions; second, we integrated all the reconstructed intensities in a box of 7 × 7 × 7 voxels around the local maxima which is the volume of an atom (2.4 × 2.4 × 2.4 $Å^3$); third, we compared all the integrated intensities of all possible atomic sites, from which we can exclude the non-atom. Specifically, we have manually removed the unphysically too close atoms, which are 112 (0.73%) atoms for Zr1, 168 (0.75%) atoms for Zr2, and 93 (0.7%) atoms for Zr3. We have added this information in the revised manuscript.

Comment 2: *Authors choose a 2 Angstrom cutoff to remove atoms from the reconstruction. This number is not explained, especially given that oxygen sites are ignored in the reconstruction. These details are the key aspects of this work.*

Response: We chose 2 Å as the cutoff based on the measurement deviation of atom positions. Since the radius of Zr is 1.6 Å, the ideal cutoff should be 3.2 Å which is the

standard Zr-Zr bond length in metal. Considering all the measurement errors due to thermal vibration and reconstruction errors, we choose the criterion of "3σ" (in statistics) to remove the outliers which are the atoms traced incorrectly. The incorrect traced atoms are unphysically too close and need to be merged.

The σ parameter is defined by the standard error of the position deviations between standard Zr-Zr bond length (3.2 Å) and the traced atoms. The σ parameter is measured by the blurring width of reconstruction volume (that is, the standard deviation of the gaussian-shaped volume of an atom) at the atom sites. The distribution of σ is 0.357 ± 0.004 Å, as Fig. R8 shows. So, the cutoff is determined to be 3.2 - 3 × 0.357 ≈ 2 Å. The similar approach for estimating σ parameter has been reported elsewhere (Chen, Z. *et al*. *Science* **372**, 826–831 (2021)).

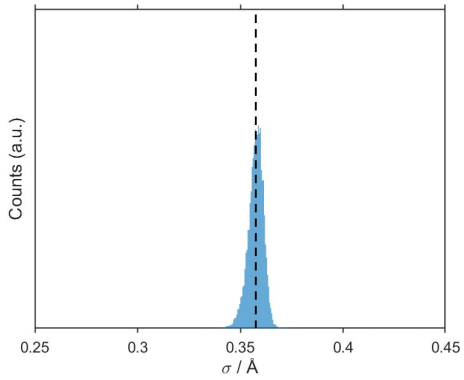

Figure R8. The blue histogram shows the distribution of parameter σ. The mean value of σ (0.357 Å) is marked by the dashed line.

Comment 3: *The authors should show the raw reconstructions in the supplemental and provide the data before and after reconstruction. The raw reconstruction needs to be provided for assessment.*

Response: The raw reconstruction volumes of Zr1, Zr2 and Zr3 are presented in Fig. R9, viewing from the [110] zone axis of the c-ZrO_2 region in Zr1 and Zr2. We have included the volume rendering of the raw reconstructions (Fig. R9 and new Supplementary Fig. 6) in the revised manuscript and provided a movie of Zr1 volume slices to view the cross sections of this volume (Supplementary Movie 5). We have uploaded our raw reconstructions (including the raw tilt series, raw reconstructions and traced atom positions along with all necessary codes) to Zenodo (https://doi.org/10.5281/zenodo.12742309). We have added this information in the revised manuscript.

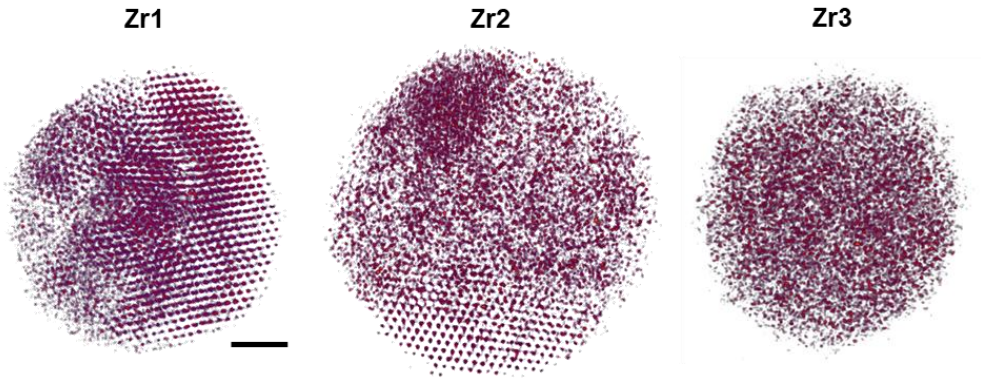

Figure R9. Volume rendering of raw reconstructions of Zr1 (left), Zr2 (middle) and Zr3 (right) NPs. Scale bar, 2 nm.

Comment 4: *Line 110: It is not appropriate to cite other tomography manuscripts for your reconstruction methods. This manuscripts novelty is primarily in the data and reconstruction, less about the scientific conclusions around ZrO.*

Response: We have removed these citations in the revised manuscript. In this study, we have computed the reconstructions using the real space iterative reconstruction (RESIRE) algorithm. We left one citation about the RESIRE at this position in the revised manuscript.

Comment 5: *The authors should analyze the raw reconstructions to show consistency with the wire diagrams in Fig 3. The interpretation of these interfaces should be clearly visible from the raw reconstruction.*

Response: We thank our referee for raising up this important point. To better illustrate the interfaces in the raw reconstruction, we present the corresponding slices of the raw reconstructed volume. Fig. R10a shows the atomic model of the semi-coherent interface corresponding to Fig. 3e. We colored the layers from top to bottom with different colors. Fig. R10b shows the layer-by-layer slices of the raw reconstruction volume with all the traced atomic positions marked by red dots. These slices show the Zr atom layer in the $(\bar{1}\bar{1}1)$ crystal plane of metal core (or in the (002) crystal plane of the oxide, as Fig. 3g shows). The red dots highlight the positions of traced Zr atoms in the slice images, which shows the consistency between the raw reconstruction and the traced atomic model. The semi-coherent interface is clearly seen from the raw reconstruction slices. In the same manner, Fig. R11 and Fig. R12 show the slices from raw reconstruction volumes at the metal/c-ZrO_2 incoherent interface (Fig. 3k) and metal/a-ZrO_2 incoherent interface (Fig. 3l), respectively.

We have added the new analysis as Supplementary Fig. 16-18 in the revised manuscript.

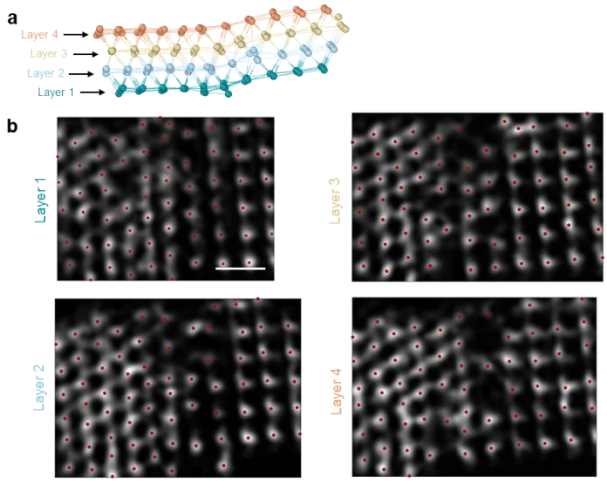

Figure R10. The raw reconstructed intensity of the semi-coherent metal/c-ZrO_2 interface. a, The atomic model of the interface, which is the same as the one in Fig. 3e. The layers are marked by different colors. **b**, The colored layers of the sliced intensity correspond to the layers in panel **a**. The red dots highlight the positions of Zr atoms. Scale bar, 2 nm.

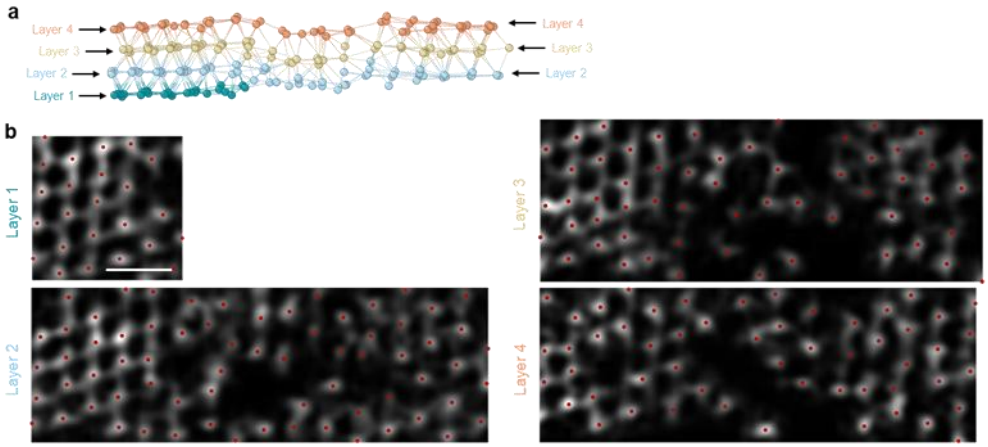

Figure R11. The raw reconstructed intensity of the incoherent metal/c-ZrO_2 interface. a, The atomic model of the interface, which is the same as the one in Fig. 3k. The layers are marked by different colors. **b**, The colored layers of the sliced intensity correspond to the layers in panel **a**. The red dots highlight the positions of Zr atoms. Scale bar, 2 nm.

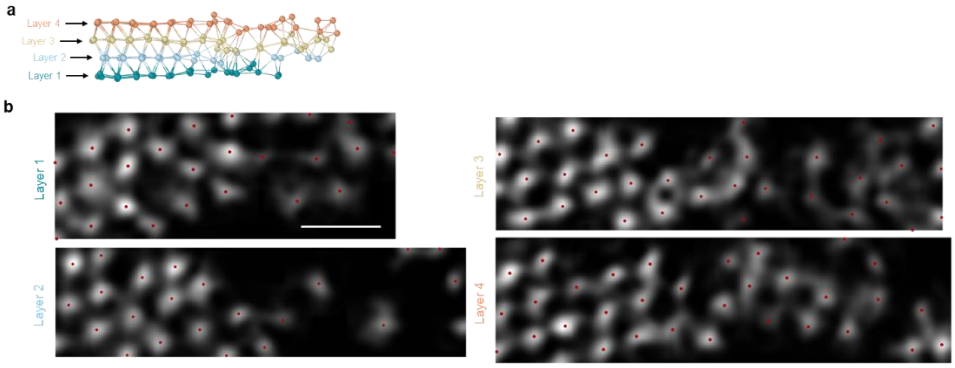

Figure R12. The raw reconstructed intensity of the incoherent metal/a-ZrO_2 interface. a, The atomic model of the interface, which is the same as the one in Fig. 3l. The layers are marked by different colors. **b**, The colored layers of the sliced intensity correspond to the layers in panel **a**. The red dots highlight the positions of Zr atoms. Scale bar, 2 nm.

Comment 6: *Atomic electron tomography suffers severely from the lack of full specimen tilt known as the missing wedge. This work has a typical missing wedge which will prevent accurate reconstruction on regions of this nanoparticle. Attempts to alleviate this have been done with machine learning (https://www.nature.com/articles/s41467-021-22204-1), however those bring in unwanted prior assumptions about crystal structure. It is not clear to the reader what parts of the atoms presented can be reliably analyzed.*

Response: This is a very good point. Iterative reconstruction algorithms such as RESIRE, GENFIRE and EST (Pham, M. *et al. Sci. Rep.* **13**, 5624 (2023); Pryor, A. *et al. Sci. Rep.* **7**,10409 (2017)) have been proved to be capable of better alleviating the missing wedge problem, comparing to WBP, SART or SIRT algorithms.

To show the effect of missing wedge and possible artifacts, we have performed the multi-slice simulation and further evaluated our reconstructions (please see response to Comment 3 of referee 1). Fig. R4b shows the simulated tilt series of the Zr1 nanoparticle. Using the same processing procedures described in the Methods section, we obtained the 3D reconstructed volume and the traced atomic coordinates from the simulation data. By comparing experimental model with multi-slice one, we estimated that 97.2% of atoms were identified correctly with a 3D precision of 28 pm (Fig. R13a). We also compare the RMSD values of the atoms in and out of missing wedge directions. There is no significant difference between the RMSD of atoms in missing wedge direction and out of missing wedge direction (Fig. R13b). The 3D precision and tracing error are similar to the previous reported results (*Nat. Mater.* **21**, 95-102 (2022); *Nature* **542**, 75-79 (2017)).

We agree with our referee that machine learning algorithms could possibly help the missing wedge problem but the associated prior assumptions could also induce unwanted errors. We have not used any machine learning in this study as there is no good training datasets of 3D reconstruction of oxides. We do not want to introduce unwanted prior assumptions in this case.

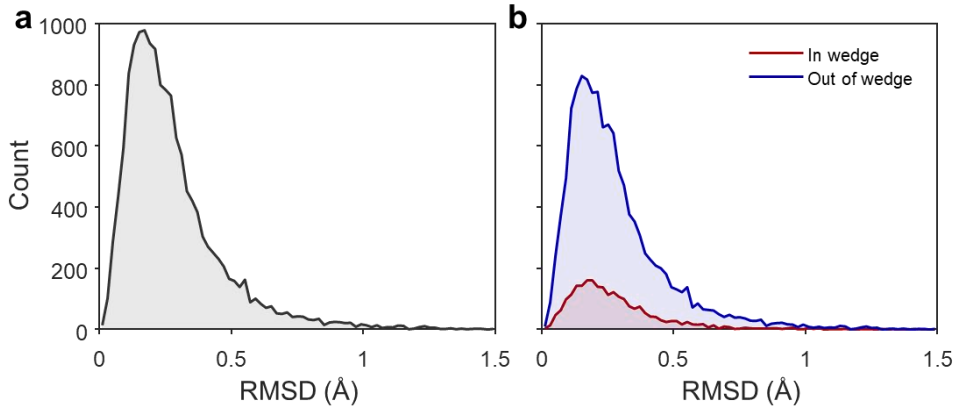

Figure R13. Comparison of experimental model with 3D multi-slice simulated model of Zr1 nanoparticles. a, Histogram of the root-mean-square deviation (RMSD) between the experimental 3D atomic model and the new 3D atomic model traced from simulated reconstructions. By comparing experimental model with multi-slice one, we estimated that 97.2% of atoms were identified correctly with a 3D precision of ~28 pm. **b**, Histogram of the RMSD of atoms in missing wedge direction, and atoms out of missing wedge direction, respectively.

Comment 7: *The authors present as though all atoms have been accurately reconstructed. However, it may be that 80-90% of the atoms are correctly identified with false positives and false negatives present. The reader will incorrectly assume that AET provides 100% accuracy. Rather, readers should understand that this accuracy is marked achievement for directly measuring atomic structure in matter.*

Response: We thank our referee for the positive comment. From the above multi-slice simulation (Fig. R13), the precision is ~28 pm; and about 97.2% atoms are correctly identified. We have included the simulation results and mentioned the inaccuracy of our 3D reconstructions in our revised manuscript.

=Self Consistency with EELS / EDX=

Comment 8: *The reconstructions seem inconsistent with the core-shell structure in S Fig1, 3. The most convincing reconstruction would be a crystalline metal core and a mostly / partially amorphous oxide shell. Why are the S. Fig1, 3 so different than the reconstructed particles (note the raw projection data in S Fig 4,5,6 do not have the same structure as S. Fig1, 3 so they may be a different type of particle).*

Response: Thanks for pointing this out. We have performed more STEM images on our Zr NPs. Variety of structural morphologies (Fig. R5) were obtained due to sample preparation method: the laser ablation. As we clarified in our response to Comment 4 of referee 1, this method can provide very high temperature to melt and vaporize metal target, and fast cooling to yield nanoparticles with large variety of morphologies including amorphous, partially amorphous and crystalline metal nanoparticles (Liang, S.-X., *et al. Phys. Chem. Chem. Phys.* **23**, 11121–11154 (2021); Tong, X., *et al. Nat. Mater.* accepted). In this study, we selected the particles with a suitable size and

various of metal-oxide interfaces to do AET experiments. We marked all the Zr NPs with similar morphology to Zr1 (Fig. R5 and Supplementary Fig. 1a).

To further confirm the partial oxidation, we take more EDS maps of a similar Zr-ZrO_2 nanoparticle with a crystalline metal core and an oxide shell (Figs. R14a–c). The line profile of Zr elemental intensity is particularly high at the core of this nanoparticle, indicating this nanoparticle has a metallic Zr core and ZrO_2 shell (Fig. R14d).

We also want to clarify that the previous EELS mapping was taken on larger particles with a different morphology as the larger particles have a much higher SNR and could give us more accurate elemental mapping. We thought it could provide some information on the partial oxidation of Zr particles although it was taken on Zr NPs with different morphology comparing to our tomographic NPs. To avoid any misunderstanding, we removed the EELS measurement in the revised manuscript (Fig. R15 shows the EELS results in the previous manuscript).

Besides, we have tried to take EDS maps on our Zr1. However, suffering from heavy carbon contaminations, the signal is too low to get a good EDS map (Fig. R16). Moreover, increasing the dose will cause damage and cause drift, unfortunately we failed to acquire a reliable EDS map on the exact original Zr1 particle for tomography.

We have added our new STEM images (Supplementary Fig. R1b) and EDS mappings (Supplementary Fig. 2) in our revised manuscript.

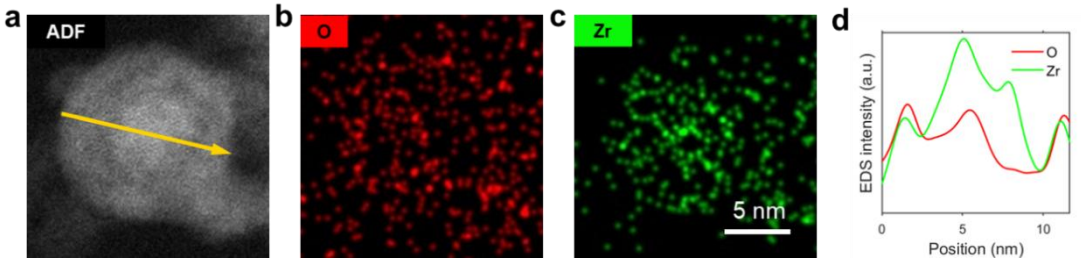

Figure R14. EDS characterization on a similar Zr-ZrO_2 nanoparticle. a, The ADF-STEM image of the Zr-ZrO_2 nanoparticle. **b**, The EDS mapping of Zr. **c**, The EDS mapping of O. **d**, The line profile along the red arrow in panel **a**. The intensity of Zr is high at the core, which shows the metal-oxide core-shell structure of this nanoparticle.

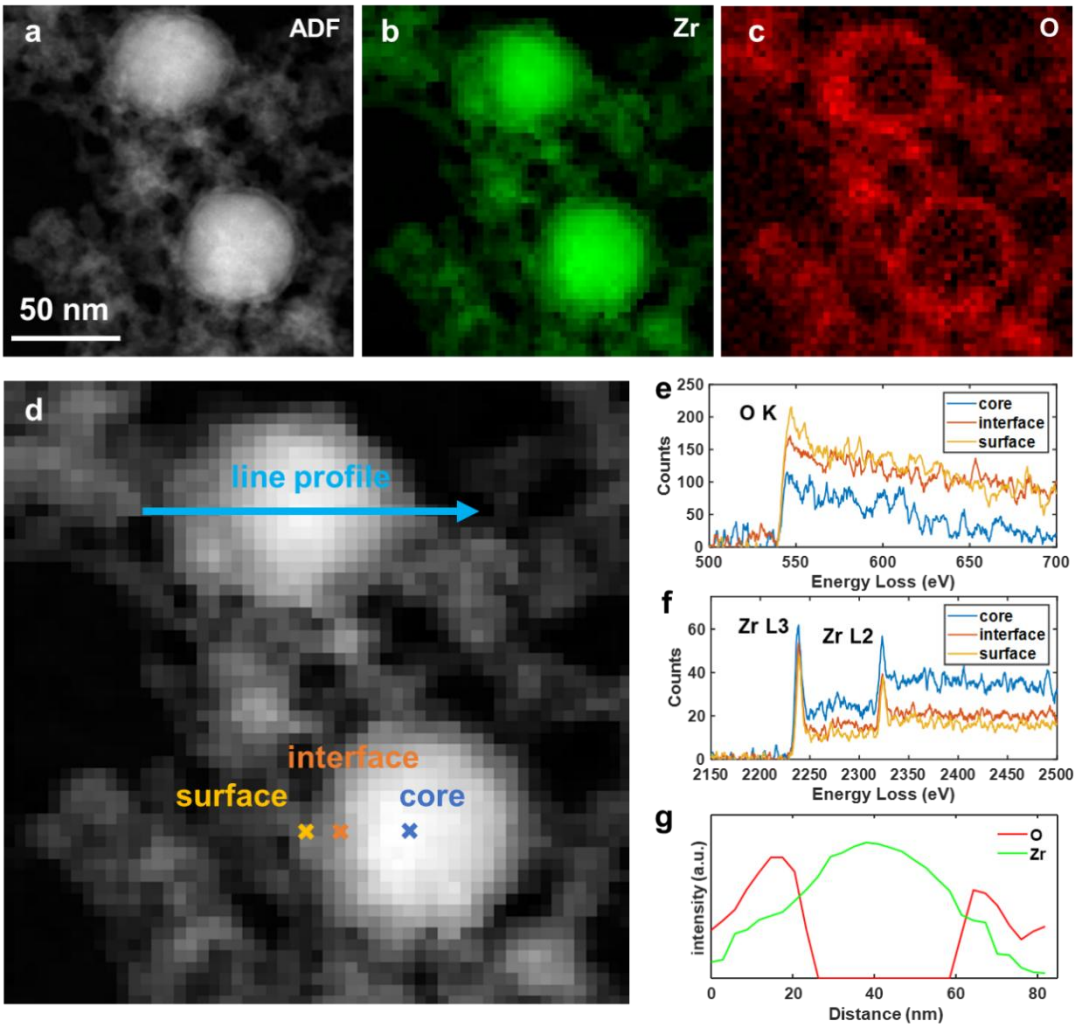

Figure R15. EELS mapping results presented in the previous manuscript. The ADF-STEM image (**a**) and its corresponding Zr (**b**), O (**c**) EELS mapping, with high Zr signals at the center of the NP and high O signals at the edge. The EELS spectrums of O (**e**) and Zr (**f**) from the points picked in (**d**) at core (blue), interface (orange) and surface (yellow). (**g**) The intensity profile of Zr and O respectively along the blue arrow in (**d**).

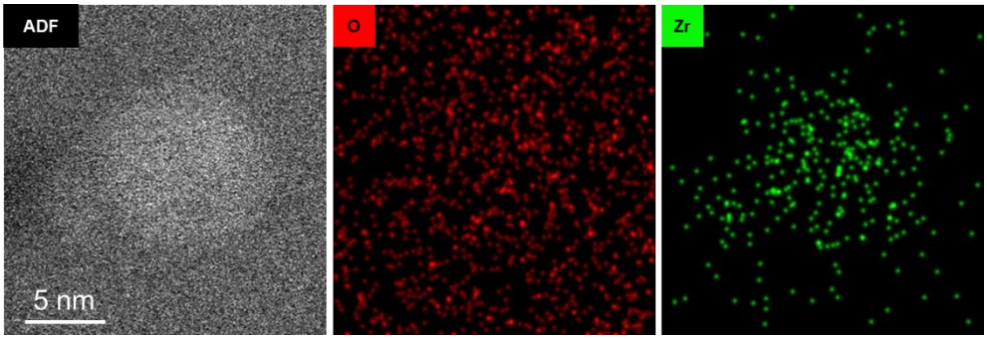

Figure R16. EDS characterization on the Zr1 nanoparticle. The ADF-STEM image (left panel) shows the heavy carbon contamination on the nanoparticle. The middle and right panel shows the O and Zr chemical mapping results with low signal.

Comment 9: *Authors claim to map oxygen indirectly from the local volume around*

metal sites. This is an interesting approach, but I am not confident it provides the resolution accuracy to conclude that oxygen metal interfaces are gradually smooth. In fact, everything else in this manuscript suggests this is not the case (the crystal to amorphous transitions, and the chemical maps in SFig 3). Chemical mapping in projection can make these assessments reasonably well and they do not appear to be in agreement. It may be prudent to not overclaim the accuracy of oxygen mapping using this method.

Response: We would like to clarify this important point. We agree with our referee that our oxygen filling approach is an indirect way of dealing the oxidation problem. From our 3D density analysis and oxygen mapping results, the interfaces are diffuse interface at a range of 10 Å (Figs. 2d & 2e). The incoherent interfaces between metal and c-ZrO_2 are more disordered, forming a crystal-amorphous-crystal interface with a thickness of ~10 Å (Fig. 3k). Moreover, the thickness metal and a-ZrO_2 is also ~10 Å (Fig. 3i). These consistent results show the thickness of interface in Zr1 is about 10 Å. To further check the structural order of the interfaces (the crystalline to amorphous regions), we calculated the normalized bond orientational order (BOO) parameters for all the atoms in the metal/a-ZrO_2 incoherent interfaces (Fig. R17a&b). We observed a gradually increased BOO from disordered a-ZrO_2 grain side to metal grain side. The BOO of incoherent interface of metal/c-ZrO_2 exhibits a gradually decreasing and then increasing (Fig. R17c&d). These results show the interfaces are gradually smooth. We have performed more EDS mappings (Figs. R14 & 17e-l) on different particles, the line profile shows the atomic fraction of Zr decreases gradually from core to surface. The gradually change of Zr concentration indicates a smooth metal oxide interface.

The EELS maps, however, were taken on much larger Zr particles and the pixel size is 30 Å (Fig. R15). From the EELS mapping, it cannot give us the information about the smooth interface with of width of 10 Å which is smaller than a single pixel size in EELS mapping. To avoid any misunderstanding, we removed the EELS measurement in the revised manuscript. We have added the new EDS results in the revised manuscript.

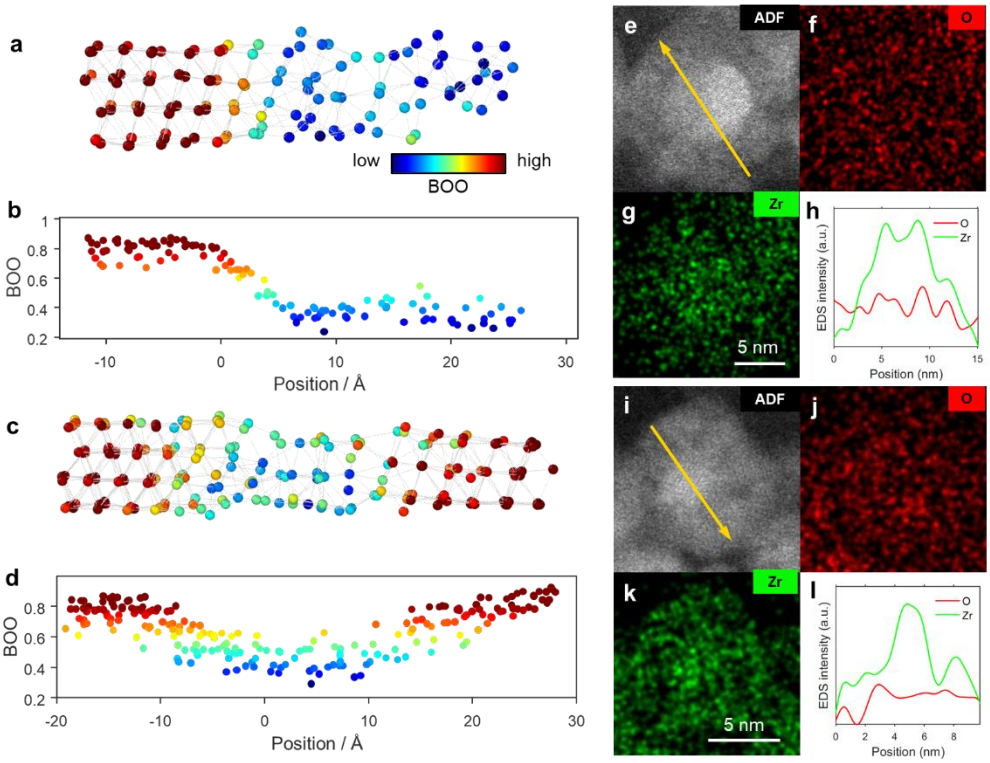

Figure R17. The gradually smooth interface structures. a-b, The normalized bond orientational order (BOO) parameters for all the atoms in the metal/a-ZrO_2 incoherent interfaces. The atoms are colored according to the BOO value (**a**). The BOO value plotted from left to right shows the thickness of the interface is ~10 Å (**b**). **c-d**, The normalized BOO parameters for all the atoms in the metal/c-ZrO_2 incoherent interfaces. The atoms are colored according to the BOO value (**c**). The BOO value plotted from left to right shows the thickness of the interface is ~10 Å (**d**). **e-h**, The ADF-STEM image (**e**) and the corresponding EDS chemical mapping of O (**f**) and Zr (**g**) show the core-shell structure of the Zr-ZrO_2 nanoparticle. The line profile (**h**) of the atomic fraction of Zr and O, along the yellow line in panel **e**. **i-l**, The ADF-STEM image (**i**) and the corresponding EDS chemical mapping of O (**j**) and Zr (**k**) show the core-shell structure of the Zr-ZrO_2 nanoparticle. The line profile (**l**) of the atomic fraction of Zr and O, along the yellow line in panel **i**. The line profiles of Zr decreases gradually from core to shell.

Comment 10: *Authors do not explain why the oxygen sites are not reconstructed. The signal from the MAADF is lower, but some oxygen scattering still occurs. Discussion here would be helpful.*

Response: We appreciate our referee for this important comment. Please refer to our response to Comment 3 of referee 1. We compared the simulation images in 2D and 3D, the oxygen signal under our experiment conditions is too weak to be detected.

Comment 11: *In Figure 4, the authors analyze voids from what appears to be the raw reconstruction. This is the correct approach. However, it is not clear if this is in fact the raw reconstruction, or if it is a reconstruction made after atoms were filtered out using the atom tracing methods. Also, is oxygen present in these voids?*

Response: Thanks for pointing this out. We show 3D surface renderings of one representative vacancy in Zr1. The raw volume rendering structures clearly indicates no Zr atom density at the vacancy site (blue site in Fig. R18a). The intensity of vacancies is much lower than the Zr atoms (Fig. R18b). As we clarified in response to Comment 3 of referee 1, our experiment and simulation results reveal the low contrast of oxygen atoms, both in 2D ADF-STEM images and 3D AET reconstruction. We cannot detect the signal of oxygen under current ADF images, but considering the intrinsic oxygenophilic nature of Zr metal, there should be the oxygen adsorption/bonding on the inner surface of these voids. The oxygen atoms can present in these voids. We have clarified that the vacancies we detected are Zr vacancy but not oxygen vacancy in our revised manuscript.

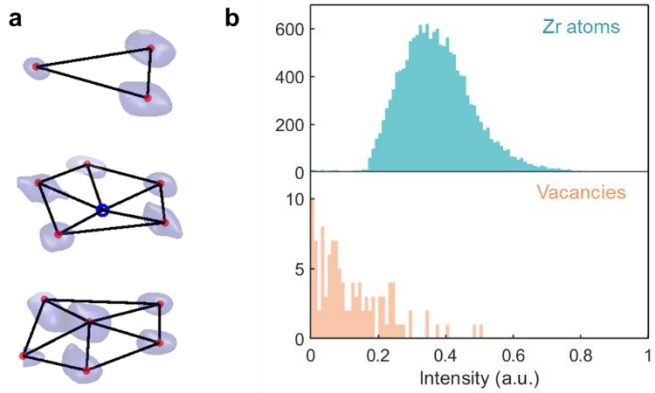

Figure R18. 3D determination of a vacancy in the Zr1 nanoparticle. a, 3D surface renderings of one representative vacancy in Zr1. The blue isosurface shows the intensity distribution of volume around the vacancy. The red dots are the positions of Zr atoms around the vacancy. The blue circle highlights the position of the Zr vacancy. **b**, The intensity histogram for all the Zr atoms (up panel) and all the vacancies (down panel) in Zr1. The intensity of vacancies is much lower than those of the Zr atoms.

=Other=

Comment 12: *The manuscript incorrectly claims to use HAADF imaging. However, the requirements for HAADF are inner collection angles 3x the convergence angle (see H. Rose). At 1.5x the convergence angle this would be medium angle ADF (MAADF). The artifacts associated with MAADF AET remain poorly known. It is unlikely to change the primary conclusions of the manuscript, but will reduce the total number of accurately reconstructed atom sites.*

Response: Thanks for pointing it out. We incorrectly claimed the HAADF imaging. We have corrected all of them to ADF-STEM. The accuracy of reconstruction under this acquisition condition has been validated by the reconstruction of tilt series generated by multi-slice simulation (Fig. R3 & R4). The simulated reconstruction shows the reliability of our reconstruction, with an atomic coordinate precision of ~28 pm and 97.2% retrieved atoms.

=Minor comments=

Comment 13: *Authors claim on Line 373, "5E5 e/A^2 is a very low dose rate" however, this is far from low dose exposures to materials. For tomographic imaging, it is about average and on par with other AET work, more broadly it would be considered higher dose.*

Response: We appreciate this very important point. Our tomographic electron dose is relatively low comparing to most of the high-resolution STEM imaging which could be ~ 10^6 e/Å^2 level (Susi, T., *et al. Phy. Rev. Lett.* **113**, 115501 (2014); Hudak, B.M. *et al. ACS Nano* **12**, 5873-5879 (2018)). It is commonly used for the AET experiments (Zhou, J. *et al. Nature* **570**, 500-503 (2019)). This dose indeed is not as low as low-dose imaging for electron beam sensitive materials. We have removed this sentence to avoid any misunderstanding.

Comment 14: *There are several minor grammatical / writing comments that are easily corrected. They do not detract from the scientific merit of this work.*
Line 32: The first sentence here should be removed.
Line 35: "oxidation processes"
Line 38: "the" Kirkendall effect
Line 43: Do the authors intend to say observation of theories? The theories are aften atomistic.
Line 64: "is limited to"
Line 66: "difficult to image"
Line 77: "tomography experiments"
Line 73: Should be "chose" not "choose"

Response: Thanks for pointing these out. We have corrected them in our revised manuscript.

REVIEWERS' COMMENTS

Reviewer #1 (Remarks to the Author):

The reviewer thanks the authors for the revision. Overall, the manuscript is well revised and the reviewer can recommend the manuscript for publication in Nature Communications.

Reviewer #3 (Remarks to the Author):

The authors have sufficiently addressed my comments. I would like to see a shortened version of their response to comment 2 (the 2 Å cutoff choice) incorporated into the methods.

Reviewer #3 (Remarks to the Author):

The authors have sufficiently addressed my comments. I would like to see a shortened version of their response to comment 2 (the 2 Å cutoff choice) incorporated into the methods.

Response: We thank referee3 for the constructive suggestions. We have incorporated the choice of the cutoff into the methods section.